

# 19TH INTERNATIONAL COSMIC RAY CONFERENCE

LA JOLLA, USA AUGUST 11-23, 1985

## CONFERENCE PAPERS



**SH**  
SESSIONS  
VOL. 4

STUDY OF NON-THERMAL PHOTON PRODUCTION UNDER DIFFERENT SCENARIOS IN SOLAR FLARES: I. SCENARIOS AND FORMULATIONS.

J. Pérez Peraza\* and M. Alvarez-M.\*

Instituto de Geofísica, UNAM, 04510, México, D. F. MEXICO

A. Gallegos

Depto. de Física, UPICSA, 08400, México, D. F., MEXICO

I. INTRODUCTION. In order to study the overall phenomenology involved in solar flares, it is necessary to understand their individual manifestation before building a corresponding description of the global phenomenon. Here we are concerned with the production of X and  $\gamma$ -rays in solar flares. Following the model in (1), flares are initiated very often within the closed magnetic field configurations of active centers. According (2) when  $\beta = \text{kinetic energy density/magnetic energy density} \geq 0.2$ , the magnetic trap configuration is destructed within the time scale of the impulsive phase of flares ( $< 100$  s). A first particle acceleration stage occurs during this phase as indicated by impulsive microwave and hard-X-rays bursts. In some flare events, when the field strength B is very high, the broken field lines may close again, such that later, in the course of the flash and main phases more hot plasma of very high conductivity is created, and so, the field and frozen plasma expand outward, as the kinetic pressure inside the closed loops increases. The magnetically trapped particles excite strong Alfvén wave turbulence of small transverse scale. According to (3), small scale turbulence of linear dimensions  $\sim (1 - 10)$  Km may account for effective stochastic acceleration up to relativistic energies. In addition, according to (4) a high pressure piston which drives a shock within the closed configuration may be formed: magnetized turbulent cells remain bounded in the wake of the "bottle up" shock wave. Since the shock moves faster than the expanding bottle, the stochastic acceleration overcomes the 1st. order Fermi process (adiabatic losses) due to the expansion of the bottle. As discussed in (4) the expanding bottle opens or not depending on whether the duration of the flare induced shock is larger or not than the Raleigh-Taylor instability grow time. Therefore, when the conditions of the opening are satisfied we expect a definite slope change in the energy spectrum, indicating two different particle populations. In the case that the magnetic trap is not destructed during the impulsive phase, because  $\beta < 0.2$ , the population of the 1st. acceleration stage mix within the expanding bottle with that of the second stage, in which case not a noticeable change in the spectrum slope is expected. On the other hand, in the case that the conditions for the opening of the expanding bottle are not remplished, but the magnetic loop of the impulsive phase was broken ( $\beta \geq 0.2$ ), only the component of the first acceleration stage will be observed. Obviously if the closed magnetic structures do not open during the impulsive phase ( $\beta < 0.2$ ) neither during the subsequent expansion in the main phase, no particle event is expected. Finally, if the flare does not occur within a closed magnetic field configuration, only one main acceleration stage is expected.

II. SCENARIOS FOR X AND  $\gamma$ -RAYS PRODUCTION. Within this context, four scenarios have been examined: (a) Production of the radiation in the source of particle acceleration during the impulsive phase, in a tick geometry context (high amount of traversed matter: high density  $n$  and/or long time  $t$ ); (b) Production of the radiation in the source of secondary particle (\*). On leave for the INAOE, Tonanzintla, 72000 Puebla, MEXICO

acceleration (tick geometry); (c) Production of the radiation during secondary acceleration by the superposition, of particles of that stage mixed with the component of the 1st. acceleration stage when  $\beta < 0.2$  (tick geometry), and (d) Production of the radiation out of the source of impulsively accelerated particles in a thin geometry context (low amount of traversed matter in the source), either in coexistence or absence of closed field structures. Though particles do not lose energy in the source, they are decelerated by Coulomb collisional losses during transport to the emission volume (dense chromosphere or coronal condensations).

III. ENERGY LOSSES OF SOLAR FLARE ELECTRONS. The main energy losses are: Coulomb-Collisional losses (CC), Bremsstrahlung (BR), Inverse Compton Effect (IC), Synchrotron Losses (SY) and Adiabatic Losses (AD). The later are negligible at low energies, becoming gradually important at high energies, however, since the acceleration rates also increase with energy, the predominance of acceleration is conserved. Therefore we have only considered (AD) losses within the frame of scenario (c), with a rate given as  $(dE/dt)_{AD} = - (2/3)(V_r/R) \beta W(eV/s)$ , where  $\beta = v/c$  is the particle velocity in terms of the light velocity  $c$ ,  $W$  is the total energy,  $V_r = 2000$  Km/s the expansion velocity and  $R = 0.7 R_\odot$  is the expanded distance, with  $R_\odot =$  the solar radius. For (SY) losses we used the next formula  $(dE/dt)_{SY} = -0.98 \times 10^{-3} B^2 (\beta^2/1-\beta^2) (eV/s)$ , however, they are only important at relatively high energies and strong magnetic fields (Fig. 1); since for the field strength prevailing in flares the electromagnetic radiation produced by synchrotron effects falls very far from the X-ray domain, for the task of simplicity we ignore them in a first approximation. Though (CC) effects do not contribute to X-ray production, energy losses are very important at low energies in determining whether or not the acceleration rate is enough high to generate energetic particles from the thermal solar plasma. Therefore the considered prevailing processes are:

$$(dE/dt)_{CC} = - \frac{K_1}{\beta} \ln \Lambda \{ K_2 [0.88 \operatorname{erf}(X_p) - 1.84 \times 10^3 X_p e^{-X_p^2}] + K_3 [0.88 \operatorname{erf}(X_e) - 2X_e e^{-X_e^2}] \} (eV/s) \quad [1]$$

where  $K_1 = 1.57 \times 10^{-35} n$ ,  $\Lambda = 4.47 \times 10^{16} \beta^2 (T/n)^{0.5}$ ,  $K_2 = 5.98 \times 10^{23}$ ,  $K_3 = 1.1 \times 10^{27}$ ,  $X_p = 2.33 \times 10^6 \beta T^{-0.5}$  and  $X_e = 5.44 \times 10^4 \beta T^{-0.5}$ , where  $T$  is the temperature ( $^\circ K$ ). For non-Relativistic (BR) we used

$$(dE/dt)_{BR} = - 4.74 \times 10^{-11} n \beta \quad [2]$$

whereas in the relativistic range we have

$$(dE/dt)_{BR} = - 1.37 \times 10^{-16} n [1n W/m_e c^2 + 0.36] W (eV/s) \quad [3]$$

where  $m_e c^2$  is the electron rest energy. For (IC) we have

$$(dE/dt)_{IC} = - 1.02 \times 10^{-25} \omega_{ph} W^2 (eV/s) \quad [4]$$

where  $\omega_{ph}$  ( $eV/cm^3$ ) is the mean photon energy density: for the photon field we have employed the local field in the flare volume due to the flare phenomenon itself, instead of the back ground photospheric field. In fact, if the photon field is computed from the black body law integrated over

all frequencies for a  $T \sim 6000$  °K, therefore,  $\omega_{ph} = 2.7 akT^5$   
 $= 5.5 \times 10^{12} \text{ eV/cm}^3$  where  $a$  and  $k$  are the Radiation Density and Boltzman constants; however when this photon field reaches a distance of  $\sim 2 \times 10^9 \text{ cm}$  where flares occur, that value falls to  $\omega_{ph} \sim 2 \times 10^{12} \text{ eV/cm}^3$  due to absorption, mainly from dispersion by electrons. On the other hand, if we considered observed radiative output at flare maximum as a lower limit of the total photon field generated in flare regions, we have according to (5) that for a typical subflare (5/IX/1973) is  $10^{27} \text{ erg/s}$ , so that adopting as typical time that of 400s for the rise and fall of X-ray data in that event, the radiative output becomes  $4 \times 10^{29} \text{ erg}$ . Therefore following (6), volumes of this kind of flares are  $(0.3-2) \times 10^{26} \text{ cm}^3$ , so that  $\omega_{ph} \geq 1.2 \times 10^{15} \text{ eV/cm}^3$ . On the other extreme, class 3 flares show radiative outputs of  $\sim 10^{32} \text{ erg}$ , so that for  $V \leq 6 \times 10^{32} \text{ cm}^3$  we obtain  $\omega_{ph} \geq 10^{16} \text{ eV/cm}^3$ . It can be appreciated from Fig. 1, that the preponderant energy loss process are (CC), at least up to 1 MeV, whereas synchrotron losses for  $B < 100$  gauss are weaker in relation to the other processes. Also it may be noted that if the photospheric photon field is considered the (BR) process is predominant over the (IC) process for  $n \geq 10^{11} \text{ cm}^{-3}$ . If the flare radiation field is considered the (IC) process dominates over the (BR) process for  $n \leq 10^{12} \text{ cm}^{-3}$ , however, in the case of small flares in very high density media  $n \geq 10^{13} \text{ cm}^{-3}$  (BR) may become dominant over (IC), (Fig. 1).

IV. ENERGY SPECTRA OF THE FLARE ELECTRONS. Source energy spectra may be derived from a steady-state continuity equation of the Fokker Planck form,

$$\frac{d}{dE} (N dE/dt) + N/\tau = q(E) \quad [5]$$

for scenarios (a) to (c) we assume that particles are accelerated from the thermal background, so that the injection spectrum  $q(E) = 0$ ; in addition, if  $N$  is the number of particles per unit energy, the solution of [5] may be reduced to the well known relation of the age-energy analogy for the differential flux

$$N(E) = N_0 e^{-t/\tau} / \tau (dE/dt) \quad (\text{particles/energy} \cdot \text{cm}^2 \text{sr s}) \quad [6]$$

where  $\tau$  may be identified with a characteristic remain time in the acceleration volume and  $N_0$  the number of local particles that participate to the acceleration process. For computation of the thermal flux we integrated the Maxwell velocity distribution from the arbitrary value  $V_a = B^2/(4\pi\rho)^{0.5}$  up to  $\infty$ , where  $\rho$  is the mass-density:

$N_0 = 1.63 \times 10^{-7} n T^{-0.5} (4.79 \times 10^{22} B^4/n + 3 \times 10^{11} T) \exp(-1.58 \times 10^{11} B^4/nT)$   
 (particles/cm<sup>2</sup>sr s). For solving eq. [6] the following equilibrium equations have been employed

$$(dE/dt) = (dE/dt)_{acc} - (dE/dt)_{CC} - (dE/dt)_{IC} \quad [7]$$

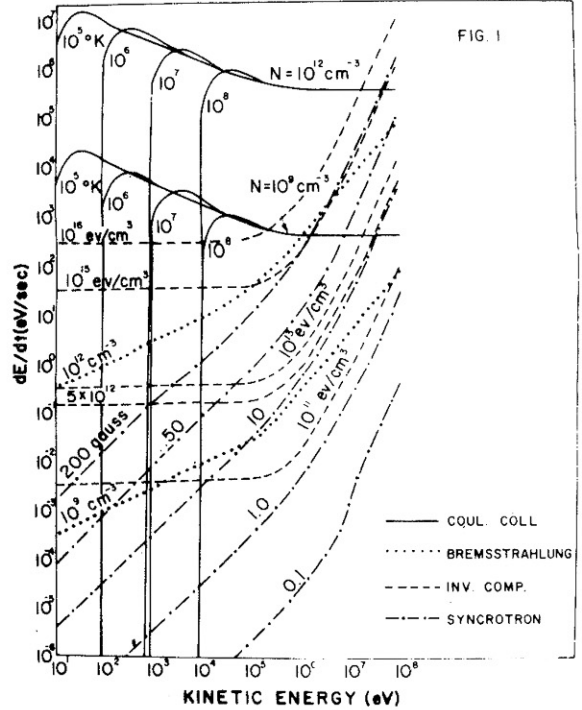
$$(dE/dt) = (dE/dt)_{acc} - (dE/dt)_{CC} - (dE/dt)_{BR} \quad [8]$$

with the exception of scenario (b) where (AD) losses have been included. Within the frame of scenario (a) two different acceleration mechanisms have been worked out: impulsive acceleration may be provided by the betatron process  $(dE/dt)_{acc} = \alpha_b \beta^2 W$  (eV/s) and electric field acceleration processes  $(dE/dt)_{acc} = ce\epsilon\beta$  (eV/s), where  $\alpha_b$  is the betatron hydromagne

ENERGY LOSSES OF ENERGETIC ELECTRONS

tic acceleration efficiency,  $\epsilon$  the electric field, and  $e$  the electron charge. For scenario (b) we employed the stochastic Fermi-type process  $(dE/dt)_{acc} = \alpha_f \beta (eV/s)$ . In scenario (c) we use the same acceleration rate that in scenario (b), and for  $N_0$  we considered the composition of two components, those of scenario (a) with spectrum  $N(E)$  and the thermal spectrum  $N_0(th)$ , in the site of secondary acceleration. For scenario (d), the general solution of eq.[5], with  $dE/dt = - (dE/dt)_{CC}$  gives

$$N(E) = \frac{e^{-t/\tau}}{(dE/dt)_{CC}} \left\{ \int_{E_{th}}^{E_{max}} q(E) e^{t/\tau} dE + N_0(th) (dE/dt)_{th} \right\} \quad [9]$$



within the frame of this scenario, the 2nd term refers to thermal particles, and so we neglected it because only the impulsively accelerated particles with injection spectrum  $q(E)$  travel to the emission region. For  $q(E)$  we considered the spectrum of neutral current sheet acceleration derived in (7), per interval time  $\tau'$ ,  $q(E) = N(E)/\tau'$ .

$$N(E) = (9.1 \times 10^{-2} n V_d / E_0) \left( \frac{E}{E_0} \right)^{-1/4} \exp[-1.12 (E/E_0)^{3/4}] \text{ (part./eV cm}^2 \text{sr s)} \quad [10]$$

where the characteristic energy value  $E_0$  and the plasma diffusion velocity  $V_d$  depend on the adopted model for neutral current sheet acceleration: for the Priest's model  $V_d = 0.057 V_a$  (cm/s) and  $E_0 = (2.75 \times 10^{18} m^{1/2} e L V_d \epsilon)^{2/3}$  (eV), where  $L$  is the scale length of the neutral sheet. The deconvolution of particle spectra in photon spectra and results are discussed in paper SH 1.2-3.

V. CONCLUSIONS. The consideration of the local photonic field of the flare instead of the conventional photospheric field, gives rise the importance of the Inverse Compton effect for the production of electromagnetic radiation by accelerated particles.

REFERENCES

- [1] Pérez-Peraza, J., Invited Talk in Proc. of the 9th. European Cosmic Ray Conference, Kosice, 1984.
- [2] Meerson, B. I. and Sasorov, P. V., adv. Space Research 1, 77, 1981.
- [3] Pérez-Peraza, J., J. Geophys. Res. 80, 3535, 1975.
- [4] Mullan, D. J., Ap. J. 269, 765, 1983.
- [5] Canfield et. al., Skylab Workshop on Solar Flares, ed. Sturrock, P., (1979)
- [6] Moore et al., Skylab Workshop on Solar Flares, ed. Sturrock, P., (1979)
- [7] Pérez-Peraza, J. et. al., Space Research 18, 365, 1978.

$$E_0 = (2.3383 \times 10^{18} m^{1/2} e L V_d \epsilon)^{2/3} \text{ MeV}$$